

Field Report: UAV-Based Volcano Observation System for Debris Flow Evacuation Alarm

Keiji Nagatani, Ryosuke Yajima, Seiga Kiribayashi, Tomoaki Izu, Hiromichi Kanai, Hiroyuki Kanasaki, Jun Minagawa and Yuji Moriyama

Abstract Once a volcano erupts, molten rocks, ash, pyroclastic flow, and debris flow can cause disasters. Debris flows can cause enormous damage over large areas. Therefore, a debris-flow simulation is an effective means of determining whether to issue an evacuation call for area residents. However, for safety purposes, restricted areas are set up around a volcano when it erupts. In these restricted areas, it is difficult to gather information such as the amount and permeability of the ash; this information is necessary for precise debris-flow simulations. To address this problem, we have developed an unmanned observation system for use in restricted areas around volcanoes. Our system is based on a multicopter micro unmanned aerial vehicle (MUAV); this system can be used to perform field tests in actual volcanic areas. In this paper, we report the field tests conducted at Mt. Unzen-Fugen during November 2016. The field tests included a demonstration of an unmanned surface flow measurement device and the deployment and retrieval of a small ground vehicle and a drop-down-type ash-depth measurement scale using an MUAV. In addition, we discuss some of the lessons learned.

K. Nagatani (✉) · R. Yajima · S. Kiribayashi
Tohoku University, 6-6-10, Aramaki-Aoba, Sendai, Japan
e-mail: keiji@ieee.org

T. Izu
ENROUTE CO., LTD., 1-3-29, Ureshino, Fujimino, Saitama, Japan
e-mail: izu@enroute.co.jp

H. Kanai · H. Kanasaki · J. Minagawa
Kokusai Kogyo Co., Ltd, 2-24-1, Harumi, Fucyu, Tokyo, Japan
e-mail: hiromichi_kanai@kk-grp.jp

Y. Moriyama
Kokusai Kogyo Co., Ltd, 2-Rokuban, Chiyoda, Tokyo, Japan
e-mail: yuji_moriyama@kk-grp.jp

1 Introduction

Recently, several active volcanoes in Japan have shown an increase in activity. In recent years, eruptions have occurred at Nishino-Shima, Kuchino-Arab, and Ontake. In the near future, there is a real possibility of a new, large-scale volcanic eruption in Japan—this includes Mt. Fuji.

Once a volcano erupts, molten rocks, ash, pyroclastic flow, and debris flow can cause disasters, as shown in Fig. 1. Debris flow is a phenomenon in which rain falls on a slope containing accumulated volcanic gravel and ash, causing them to flow downward. This can result in enormous damage over a large area. For example, in the 1990s, Shimabara City suffered damage from debris flow caused by Mt. Unzen-Fugen's eruption [1].

A debris-flow simulation is an effective means of determining whether to issue an evacuation call for residents. However, for safety reasons, a restricted area is set around a volcano when it erupts. Therefore, in the restricted area, it is difficult to gather the information necessary for a precise simulation, such as the amount and permeability of the ash. In the Mt. Shinmoe eruption in 2011, the mountain was covered with coarse volcanic sediment that made debris flow less likely; however, there was no opportunity to observe it because of the restricted area. Thus, when a small amount of rain fell and no debris flow occurred, conservative evacuation calls were made and area residents gradually disbelieved the alarm.

For a precise debris-flow simulation, direct measurements of the (A) topography shape, (B) amount of ash fall, (C) permeability of volcanic ash, and (D) rainfall are required. Therefore, since 2014, our group has been developing an unmanned observation system for use in restricted volcanic areas; the system is based on multirotor micro unmanned aerial vehicles (MUAVs). The MUAV includes a camera system to obtain images and to generate 3D terrain information, as well as a soil sampling device suspended from the MUAV [2]. In this research, we developed devices and

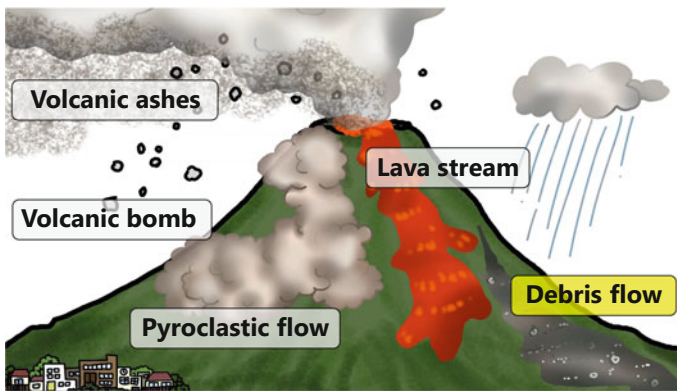


Fig. 1 Types of volcanic disasters

functions, evaluated them in real volcanic environments, and improved them on the basis of the results of the field tests.

In this paper, we report the findings of the field tests conducted at Mt. Unzen-Fugen during November 2016. The tests included demonstrations of the following:

1. A drop-down-type ash-depth measurement scale to obtain the amount of ash fall,
2. A surface flow measurement device to estimate the permeability of volcanic ash, and
3. MUAV-based deployment and recovery of a small ground vehicle that measures the amount of rainfall.

In addition, we discuss some of the lessons learned.

2 Related Works

There have been several attempts to use robotic technology for the remote observation of restricted areas. Many of them used mobile robots. Carnegie Mellon University has conducted volcanic explorations using legged robots named Dante and Dante II [3]. In Europe, a wheeled volcano exploration robot was developed by the Italian-led RoboVolc Project and tested it at Mount Etna and Vulcano Island [4]. In Japan, Tohoku University developed a teleoperated robot called Mobile Observatory for Volcanic Eruption (MOVE) [5]. The above robots were relatively large, and their operation areas were limited because of traversability problems. As a solution, some research institutes considered aerial robots. One famous example was an autonomous helicopter known as Yamaha R-Max [6]. When Mount Usu erupted in Hokkaido in 2000, an unmanned helicopter, equipped with GPS and a video camera, was employed to observe the land features and geological status in the vicinity of the crater. To obtain the advantages of both mobile robots and aerial robots, we proposed a method that combined a mobile robot and an aerial robot to observe restricted areas [7]. In the current paper, we introduce the next version of the mobile robot, which is carried by an MUAV.

3 Drop-Down-Type Ash-Depth Measurement Scale

3.1 *Ash-Depth Measurement Method*

For a precise debris-flow simulation, the direct measurement of the amount of ash fall is very important. However, it is difficult to estimate the amount of ash fall using only the visual information obtained from MUAVs. If there are many vertical scale poles in the target environment as references, it is possible to measure the ash depth by reading the values of those scales. Unfortunately, in most cases, locating such instruments on volcanoes is prohibited in Japan.

To measure ash depth, we propose a simple drop-down-type pyramid-shaped scale. In the initial stage of a volcanic eruption, or when eruption signs have been detected, an MUAV carries the drop-down-type scales to the restricted area and drops them.

After the volcanic eruption, another MUAV flies to the same location and hovers to take a photograph of the scales. Once the size and color of each scale are known, we can estimate the ash depth by detecting the visible scales.

3.2 *Prototype of the Ash-Depth Measurement Scales*

For our initial tests, we produced scales in three sizes. Figure 2a shows the prototype scales. To eliminate the need to retrieve them later, we used biodegradable plastics to construct the scales. When the ash depth is less than 1 cm, the vision sensor on the robot can see the minimum size of the scales from the sky. When the ash depth is between 1 and 2 cm, the minimum scales are not visible in the photograph, but the other two scales can be seen from the sky, as shown in Fig. 2b. When the ash depth is over 3 cm, only the largest scale can be seen from the sky.

To deploy the scales in a target environment, we developed a drop-down device (i.e., an ash-depth measurement scale). When the MUAV arrives at the target position, the device opens at the bottom and drops the scales from the air. The device has three chambers so that it can deploy the scales to three positions in one flight. A concept image of the deployment is shown in Fig. 2c.

3.3 *Initial Tests of the Ash-Depth Measurement Scale and Lessons Learned*

We conducted some recognition tests to understand the suitable conditions for the recognition of the scales. Red-, yellow-, and blue-colored 1-cm scales were manually

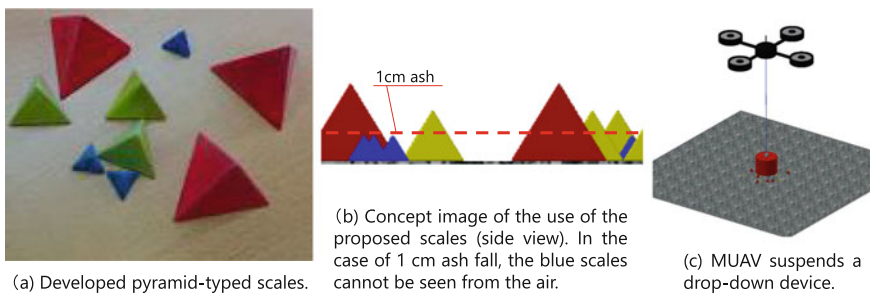


Fig. 2 Prototype of the ash-depth measurement scale, method of operation, and deployment image

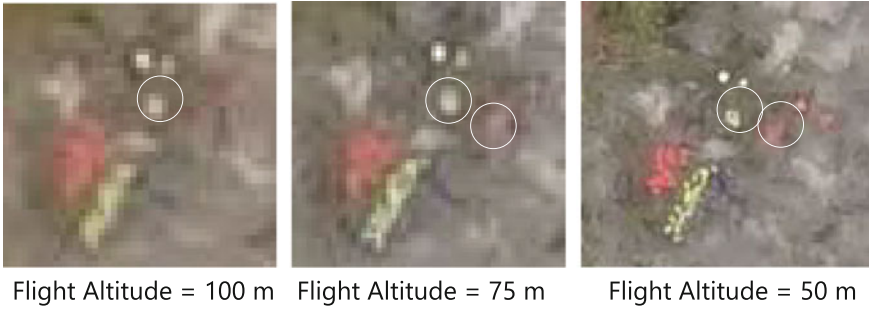


Fig. 3 Scale images from an MUAV obtained at different flight heights

deployed on the ground. The MUAV then took pictures from different flight heights. A 4000×6000 -pixel camera with a resolution of 350 dpi was used.

Test results showed that visual recognition of the scales required a height of 50 m or less. Figure 3 shows scale images obtained at different flight heights. Moreover, the order of the color visibility was (1) yellow, (2) red, and (3) blue. It was difficult to distinguish the yellow scale from other objects, such as vegetation or small waterfalls. On the other hand, blue-colored scales were difficult to recognize from above 50 m. Furthermore, when volcanic ash was spilled on the scales manually, the top of the scales was viewed as we expected.

In addition, we tested the deployment by an MUAV at Mt. Unzen-Fugen. The MUAV suspended the developed drop-down device, which was able to deliver different sizes of scales autonomously.

On the basis of the above tests, several lessons were learned.

1. The pyramid-shaped scales are suitable for measurement of the ash depth. Other shapes, e.g., rectangular shapes, were difficult to observe after the ash fell.
2. We need to consider the relationship between the camera's view angle and the positioning errors of the MUAV. The lower the MUAV flies, the better the resolution of the obtained scale image is. However, because of GPS positioning error, the target scales may be out of range when the MUAV flies lower. It may be better to fly the MUAV in a spiral fashion to obtain images reliably.
3. The scales' color should be chosen on the basis of the color of the target ground. Therefore, we should execute the following procedure for practical use.
 - a. An MUAV with a camera flies to obtain 3D terrain information of the target area. On the basis of this information, the operator determines the scale deployment locations and the optimal scale color.
 - b. An MUAV with a suspended drop-down device flies to deploy pyramid-shaped scales to the planned locations.
 - c. At regular intervals, e.g., every 2 days, an MUAV with a camera flies to obtain images of the deployed scales for measurement of ash depth.

In future field tests, we will consider the above topics and conduct the above procedure as a preparatory exercise.

4 Surface Flow Measurement Device

4.1 Development of the Surface Flow Measurement Device

Debris-flow simulations also require information on the permeability of volcanic ash. However, typical methods of measuring the permeability require manual measurement, a heavy device, an excess amount of water, and time. It is impossible to conduct the same procedure with an unmanned MUAV system. Therefore, we had to change our strategy. To improve the simulation results, we developed a surface flow measurement device to roughly estimate the permeability, instead of measuring the permeability directly.

Figure 4 shows the developed surface flow measurement device and how it works. It consists of a water storage, a controller to detect the landings and to make the water flow, two cameras, and legs. When the device detects a landing, the controller activates a servo motor to move a cutter blade to break the mounted water balloon. Then, water falls to the ground immediately as a simulation of heavy rain. The simulated rain's intensity is equivalent to 1700 mm/h. Finally, two cameras located on opposite sides of the device record the rate of water absorption into the ground. The device is 350 mm in both width and length, and 320 mm in height. The diameter

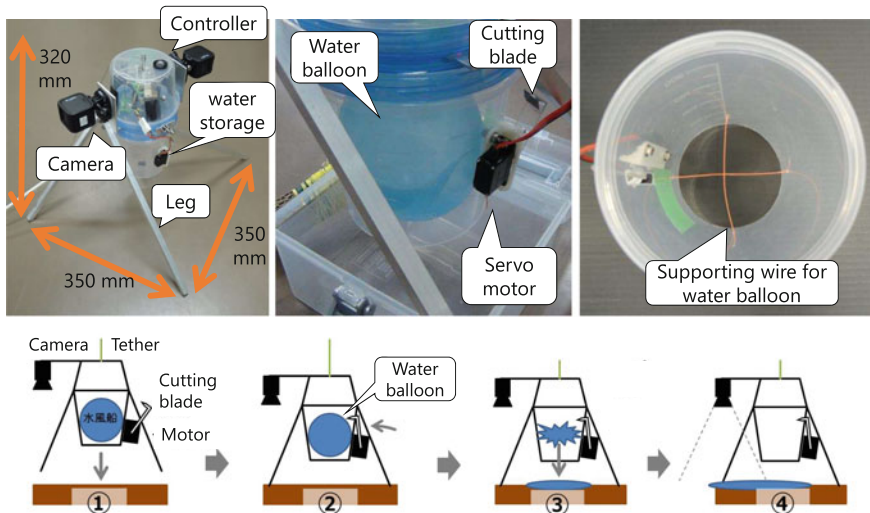


Fig. 4 The developed surface flow measurement device and its method of operation

of the storage of the water balloon is 100 mm. The maximum capacity of the water balloon is approximately 500 mL. A servo motor with a cutter blade for breaking the water balloon is located on the side of the device.

4.2 Initial Tests of the Surface Flow Measurement Device and Lessons Learned

First, we conducted initial tests without the MUAV, using deposited sand from three locations: Mt. Tarumae, Mt. Unzen-Fugen, and Mt. Sakurajima. Figure 5 shows images captured after water had fallen. In the case of volcanic ash with high permeability (Fig. 5a, b), fallen water permeated the soil quickly and the soil formed a crater shape. On the other hand, in the case of volcanic ash with low permeability (Fig. 5c), the initial fallen water let the fine particles dance like a snowstorm and then it temporarily generated a surface flow; finally, it formed an amorphous shape. The above phenomena were observed by wide-angle video cameras (GoPro) mounted on the device; the permeation time could also be measured.

Next, the water permeability coefficients of the target samples were measured by indoor experiments according to a conventional method. The results were as follows:

- Mt. Tarumae — 6.31×10^{-4} (m/s),
- Mt. Unzen-Fugen — 7.96×10^{-5} (m/s),
- Mt. Sakurajima — 1.34×10^{-5} (m/s).

The above results qualitatively matched the results obtained by the proposed surface flow measurement device.

Finally, at Mt. Unzen-Fugen, we tested the deployment of the device by the MUAV. The device was suspended by the MUAV and carried to the target position; it then landed on the ground and obtained a video clip of the surface flow of the water autonomously (Fig. 6).

During the above tests, several lessons were learned.

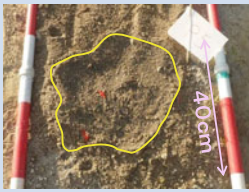


Soil	(a) Mt. Tarumae	(b) Mt. Unzen-Fugen	(c) Mt. Sakurajima
Images			
Shapes	Crater shape	Crater shape	Amorphous shape

Fig. 5 Images captured after water had fallen onto different deposited sands

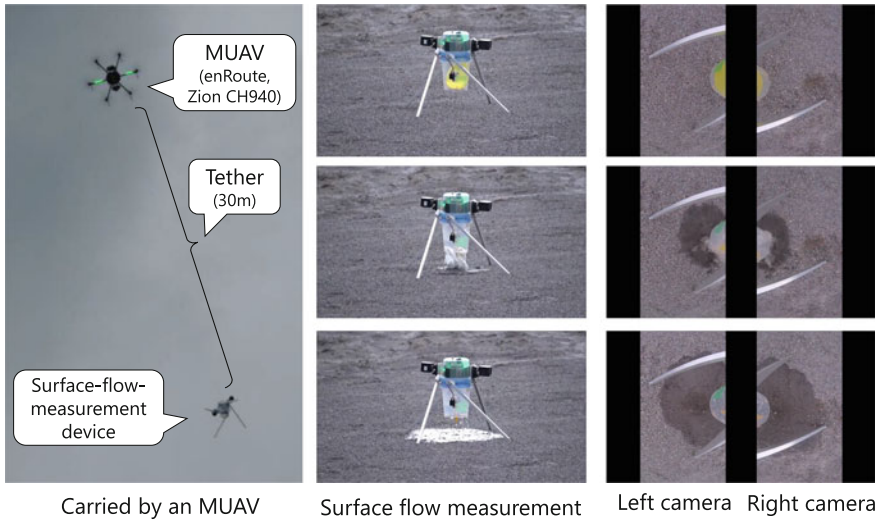


Fig. 6 Flight test of the surface flow measurement device

1. Surface flow measurement devices cannot measure strict permeability. Therefore, we will roughly classify the permeability of the soil by type, e.g., Tarumae type or Sakurajima type. In debris-flow simulations, we will use representative permeability values for each type. For classification, it is necessary to conduct additional experiments on different types of soil.
2. In the above test, we considered the size and shape of the region where water was absorbed. However, we should also consider how long it takes for the water to be absorbed.
3. We need to improve the shape of the device and its components. Once the MUAV became airborne, the tether caught the camera and the posture of the device tilted. Moreover, during the preparations for the test, the water balloon occasionally burst before being set in the device. In general, preparation of the water balloon is very troublesome.

In future works, we will redesign the device and conduct many tests to obtain data for soil classification.

5 Mobile Sensing Device Carried by an MUAV

5.1 Development of a Small-Sized Mobile Robot

The amount of rainfall is also important for precise debris-flow simulations. Continuous measurements in volcanic areas are required to estimate how much water

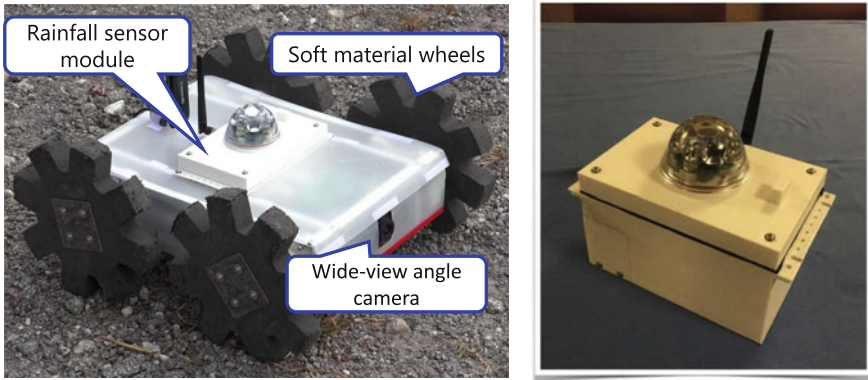


Fig. 7 CLOVER-II (left) and a lightweight rainfall sensor module (right)

the ground absorbs. However, in volcanic eruptions, sensors already installed in such areas may malfunction. In the eruptions that occurred at Mt. Unzen-Fugen in the 1990s, almost all sensors were broken. Therefore, sensors that can be installed after an eruption are needed. To install sensors at suitable positions, we developed a deployment system using a mobile robot carried by an MUAV. The robot has the capability to mount lightweight sensors.

Figure 7-(left) shows the mobile robot called CLOVER-II. It is a next-generation version of CLOVER-I, which was designed for observing volcanic environments. It can be deployed by an MUAV using the sky-crane method [7]. It has space to mount a device at its center. The robot is 400 mm in width, 465 mm in length, and 220 mm in height. The robot’s weight is approximately 3.5 kg with batteries and without sensors.

5.2 Development of a Lightweight Rainfall Sensor for a Mobile Robot

In this project, we designed and developed a rainfall sensor module to measure not only the amount of rainfall but also the barometric pressure and frequency of thunder. Figure 7-(right) shows an image of the sensor module. The sensor module includes the following three sensors:

1. Optical rain gauge
To measure the amount of rainfall, we chose an optical rain gauge (GR-11, HYDREON Corporation). Infrared light emissions inside the dome decay when raindrops attach to the surface of the dome. The amount of rainfall can be estimated according to the amount of decay.
2. Thunder sensor
A portable, commercial thunder sensor, whose chip is AS3935 (Austria Micro

Systems), is also installed in the module. It detects a signal generated by thunder or an intercloud discharge.

3. Barometric pressure sensor

A prototype of the MEMS pressure sensor, developed by Murata Manufacturing Co. Ltd., is also installed in the module. The temperature drift of the pressure sensor is smaller than that of other MEMS pressure sensors, and the noise level is relatively low.

5.3 Deployment/Retrieval Sequence of a Small Robot by an MUAV

To carry a small mobile robot in restricted areas, we propose a method for deploying and retrieving small robots using a capturing net suspended from an MUAV. The capturing net is pyramid shaped and is dropped to the ground to allow the deployment/retrieval of the robot. The size of the net is 600×600 mm, and the height is 500 mm. Figure 8 shows the deployment/retrieval sequence for the small robot. After the capturing net lands on the ground, the robot moves off the net and travels to a suitable position based on its teleoperation; it then performs a long-term fixed-point observation. After a certain period has passed, e.g., 2 weeks, the MUAV flies to the position again to retrieve the robot. The retrieval process is the reverse of the process shown in Fig. 8.

5.4 Initial Test of Mobile Robot Retrieval by an MUAV and Lessons Learned

We tested the multirotor MUAV's deployment/retrieval of the mobile robot at a mud control dam at Mt. Unzen-Fugen during November 2016. Figure 9 shows the mobile robot retrieval sequence performed by the multirotor MUAV. The multirotor MUAV

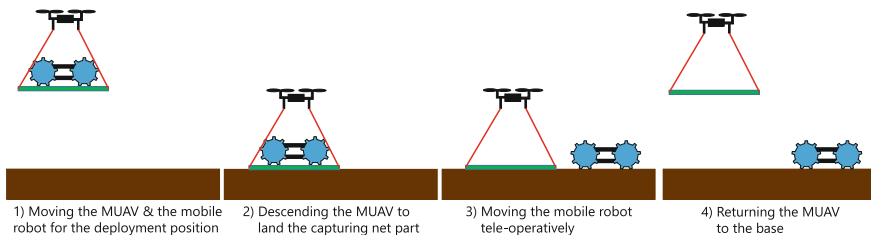


Fig. 8 Mobile robot deployment sequence as performed by the multirotor MUAV. The retrieval sequence is performed in reverse order

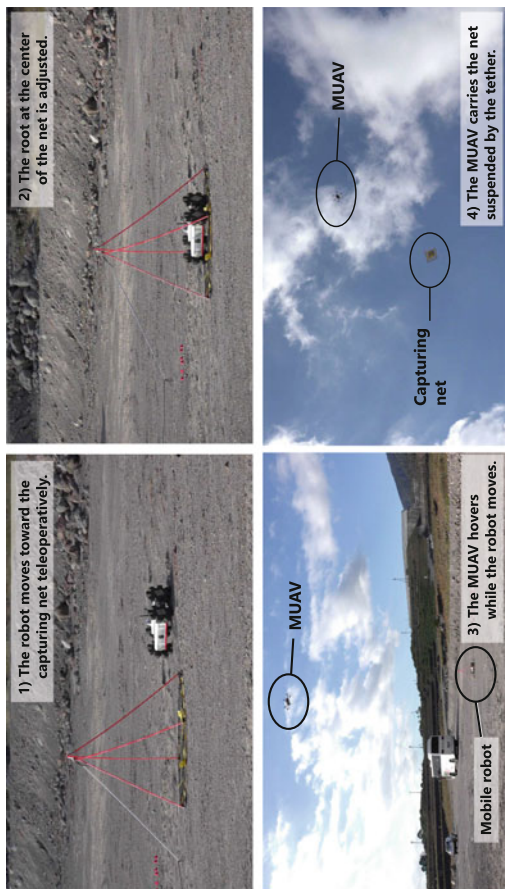


Fig. 9 Mobile robot retrieval sequence as performed by the multirotor MUAV

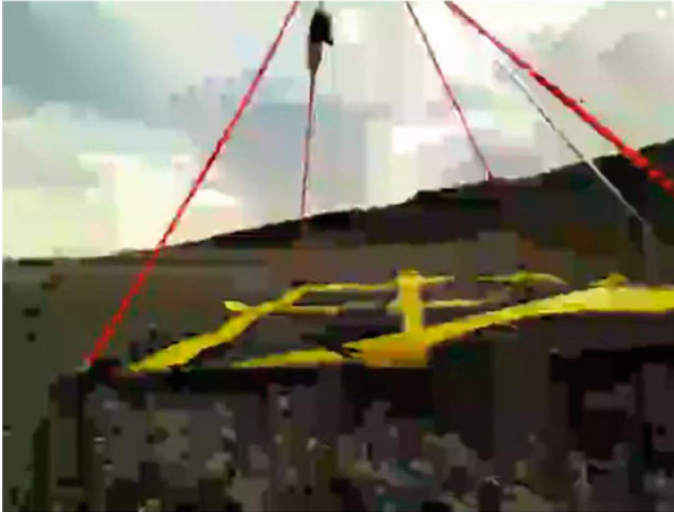


Fig. 10 A highly compressed rough image with block noise sent from the robot

hovers at the target position based on the GPS information and releases the capturing net so that it falls to the ground (upper left of Fig. 9). The teleoperated mobile robot remains near the landing point of the capturing net. After the net lands, the operator instructs the robot to move onto the center of the capturing net, using the visual information obtained by the front camera of the robot (upper right of Fig. 9). During this procedure, the MUAV hovers in the air (lower left of Fig. 9). After a certain period, the MUAV flies back to the departure point after suspending the capturing net and the robot (lower right of Fig. 9).

According to our results, the success of the above retrieval operation depends on a successful teleoperation to the center of the capturing net within a certain time, and it relies on images from the front camera of the robot. In the above case, wireless communication was the bottleneck. The small robot uses 4G/LTE to transmit its images. In typical communication situations, it sends 640×480 images at approximately four frames per second (fps) without difficulty. However, when the small mobile robot traversed the surface of the mud control dam, its antenna was located in a very low position. Therefore, the position of its electric signal was lowered, and it could send only highly compressed rough images with block noise to the operator at 1 fps, as shown in Fig. 10. As a result, the operator suffered great difficulty during the teleoperation. In this test, the robot was successfully navigated to the center of the capturing net. However, we confirmed that communication near ground surfaces is a serious problem.

6 Conclusion and Future Works

In this paper, we introduced some unmanned technologies to observe restricted areas near volcanoes and reported the results of the field tests conducted at Mt. Unzen-Fugen during November 2016. The field tests included a demonstration of (1) a drop-down-type ash-depth measurement scale for obtaining the amount of ash fall, (2) a surface flow measurement device for estimating the permeability of volcanic ash, and (3) an MUAV-based deployment/retrieval of a small ground vehicle for carrying a sensing module that includes a device for measuring the amount of rainfall. In addition, we reported some lessons learned.

As stated in the Introduction, the aim of this research was to realize a precise debris-flow simulation. Therefore, we are developing software to perform flow rate calculations and data conversions from unmanned observation data. Planned future works include developing a debris-flow simulation based on robotic devices and evaluating the simulation results.

Acknowledgements The New Energy and Industrial Technology Development Organization (NEDO) of Japan supported this work.

References

1. Setsuya, N., Toshitsugu, F.: Preliminary report on the activity at Unzen Volcano (Japan) November 1990–November 1991. *J. Volcanol. Geotherm. Res.*, ORNL/TM-12410:310–333 (1993)
2. Ryosuke, Y., Keiji, N., Kazuya, Y.: Development and field testing of uav-based sampling devices for obtaining volcanic products. In: *Proceedings of the 2014 IEEE Int'l Workshop on Safety, Security and Rescue Robotics*, October (2014)
3. Bares, J.E., Wettergreen, D.S.: Dante II: technical description, results, and lessons learned. *Int. J. Robot. Res.* **18**(7), 621–649 (1999)
4. Muscato, G., Caltabiano, D., Guccione, S., Longo, D., Coltelli, M., Cristaldi, A., Pecora, E., Sacco, V., Sim, P., Virk, G.S., et al.: Robovolc: a robot for volcano exploration result of first test campaign. *Indust. Robot Int. J.* **30**(3), 231–242 (2003)
5. Keiji, N.: Review: Recent trends and issues of volcanic disaster response with mobile robots. *J. Robot. Mech.* **26**(4), 436–441, August (2014)
6. Sato, A.: The rmax Helicopter uav. Technical Report, DTIC Document (2003)
7. Keiji, N., Kazunari, A., Genki, Y., Kenta, Y., Yasushi, H., Shin'ichi, Y., Tetsuya, I., Randy, M.: Development and field test of teleoperated mobile robots for active volcano observation. In: *Intelligent Robots and Systems (IROS 2014)*, 2014 IEEE/RSJ International Conference on. pp. 1932–1937. IEEE (2014)